

Disorder persistent transparency within the bandgap of a periodic array of acoustic Helmholtz resonators

O. Richoux, A. Maurel, and V. Pagneux

Citation: [Journal of Applied Physics](#) **117**, 104902 (2015); doi: 10.1063/1.4914184

View online: <http://dx.doi.org/10.1063/1.4914184>

View Table of Contents: <http://scitation.aip.org/content/aip/journal/jap/117/10?ver=pdfcov>

Published by the [AIP Publishing](#)

Articles you may be interested in

[Extraordinary acoustic transmission mediated by Helmholtz resonators](#)

AIP Advances **4**, 077132 (2014); 10.1063/1.4891849

[Acoustical “transparency” induced by local resonance in Bragg bandgaps](#)

J. Appl. Phys. **115**, 044913 (2014); 10.1063/1.4863400

[Wave propagation in a duct with a periodic Helmholtz resonators array](#)

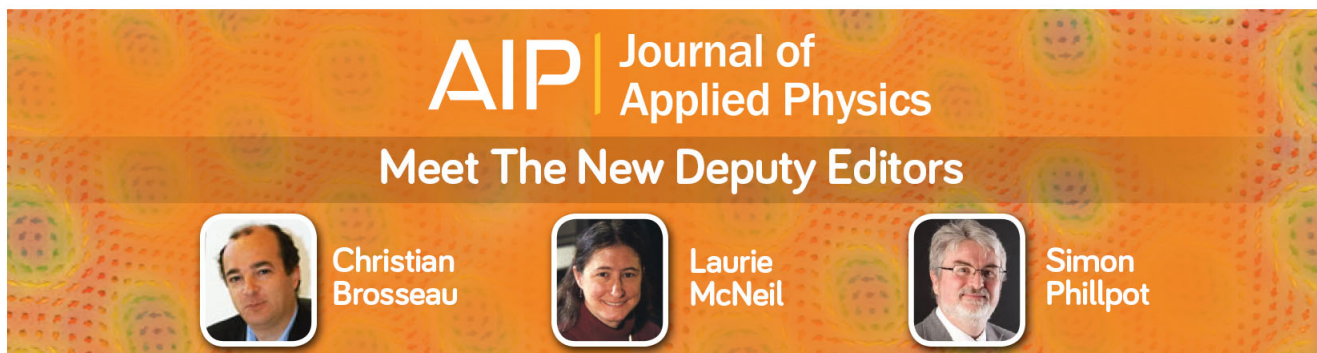
J. Acoust. Soc. Am. **131**, 1172 (2012); 10.1121/1.3672692

[Compact acoustic bandgap material based on a subwavelength collection of detuned Helmholtz resonators](#)

J. Appl. Phys. **109**, 114903 (2011); 10.1063/1.3595677

[A theoretical model to predict the low-frequency sound absorption of a Helmholtz resonator array](#)

J. Acoust. Soc. Am. **119**, 1933 (2006); 10.1121/1.2177568

A promotional banner for the Journal of Applied Physics. It features the AIP logo and the text 'Journal of Applied Physics' at the top. Below this, it says 'Meet The New Deputy Editors'. Three circular portraits of the new deputy editors are shown: Christian Brosseau, Laurie McNeil, and Simon Phillpot, each with their name written below their portrait.

AIP | Journal of Applied Physics

Meet The New Deputy Editors

 Christian Brosseau

 Laurie McNeil

 Simon Phillpot

Disorder persistent transparency within the bandgap of a periodic array of acoustic Helmholtz resonators

O. Richoux,¹ A. Maurel,² and V. Pagneux¹

¹LUNAM Université, Université du Maine, CNRS, LAUM, UMR 6613, Av. O. Messiaen, 72085 Le Mans, France

²Institut Langevin, LOA, CNRS 7587, ESPCI, 1 rue Jussieu, 75005 Paris, France

(Received 25 August 2014; accepted 24 February 2015; published online 11 March 2015)

In this paper, the influence of disorder on 1D periodic lattice of resonant scatterers is inspected. These latter have multiple resonance frequencies which produce band gaps in the transmission spectrum. One peculiarity of the presented system is that it is chosen with a nearly perfect overlap between the Bragg and the second hybridization band gaps. In the case of a perfectly ordered lattice, and around this overlap, this produces a narrow transparency band within a large second bandgap. As expected, the effect of the disorder is generally to increase the width of the band gaps. Nevertheless, the transparency band appears to be robust with respect to an increase in the disorder. In this paper, we study this effect by means of experimental investigations and numerical simulations. © 2015 AIP Publishing LLC. [<http://dx.doi.org/10.1063/1.4914184>]

I. INTRODUCTION

Phononic crystals have experienced an increasing interest in recent years because of their potential applications to acoustic filters,¹ the control of vibration isolation,² noise suppression, and the possibility of building new transducers;³ for a review, see Ref. 4. It is thus of interest to understand which properties of such structures are sensitive to inherent imperfections in their design and which are not. Besides, one can also address the question of whether or not the disorder can make new interesting properties appear.

It is usual to characterize a random medium in terms of an effective-homogeneous-medium. For random perturbation of homogeneous free space, one finds that the dispersion relation $K(\omega)$ departs from the dispersion relation $k(\omega)$ in free space without disorder, and the imaginary part of the effective wavenumber K indicates how much the opacity due to disorder is important.⁵ In the case of photonic or phononic crystals, the band structure of the unperturbed medium is more complicated, with the wavenumber Q of the Bloch Floquet mode being either purely real (pass band) or complex (stop band). The addition of disorder modifies the band structures of these periodic-on-average systems,^{6–12} and generally, produces an increase in the band gap width.¹³ Among periodic media, the case of periodic arrays of resonant scatterers is very attractive since the resonances inherent to the individual scatterers produce strong modifications of the wave propagation; these modifications in the wave properties may help in the design of materials with unusual properties. Such arrays present band gaps around the resonance frequencies of an individual scatterer. Because the scatterers are periodically located, Bragg resonances are also produced, resulting in a complex band gap structure.

Overlapping two types of gaps, a resonant scatterer gap and a Bragg gap have been shown to produce interesting phenomena (see Ref. 14 in optics and Ref. 15 in acoustics). In the case of exact overlap, a super wide and strongly attenuating band gap is predicted theoretically and shown

experimentally (firstly studied in acoustics,^{16,17} for elastic waves,¹⁸ and for microwave propagation¹⁹). When the overlap is not exact (the frequencies characterizing the different gaps are not equal) and with a small detuning, a narrow propagating band appears characterizing a slow wave feature. In recent years, this phenomenon, studied in different branches of physics, has known a revival of interest for sound isolation and slow wave application (see Ref. 20 for a review).

In this paper, we consider the propagation of an acoustic wave in a periodic array of Helmholtz resonators connected to a duct in the plane wave regime (low frequency regime with one propagating mode in the duct). The corresponding model describes the 1D propagation of the pressure field $p(x)$ through resonant point scatterers (Kronig-Penney system)^{21,22}

$$p'' + k^2 p = \sum_j V_j(k) \delta(x - jd) p(x), \quad (1)$$

where $k = \omega/c_0$ (the time dependence $e^{-i\omega t}$ is omitted, ω is the angular frequency, and c_0 the sound velocity in free space). d is the periodicity of the array and $V_j(k)$ encapsulates the effect of the j th resonator. The disorder is introduced by varying the volume of the Helmholtz resonators and thus V_j . When an overlap between a Bragg gap and a resonant band gap is produced, a narrow transparency band appears within the resulting large band gap. Unexpectedly, we found that this transparency band is robust with respect to the disorder. Indeed, first, for small disorder, the transmission decreases; but increasing the disorder further induces an increase in the transmission. We have carried out experiments whose results show qualitatively this behavior. To get further information, with a broader range of the disorder parameter, numerical calculations are shown, and they confirm the transparency induced by disorder. The paper is organized as follows: in Sec. II, the 1D model and the Coherent Potential Approximation (CPA) results for the randomly perturbed system are discussed. The experimental results are

presented in Sec. III, and this is completed by numerical calculations, in Sec. IV. Finally, a discussion is proposed in Sec. V. Technical calculations are collected in Appendixes.

II. PROPAGATION IN 1D PERIODIC AND PERTURBED HR ARRAY

At low frequencies, when only one mode can propagate in the duct, the propagation of acoustic waves in an array of Helmholtz resonators periodically located with spacing d (Fig. 1) can be described by Eq. (1). The potential $V_j(k)$ describing the effect of the j th resonator is (details are given in Appendix A)

$$V_j(k) = -\frac{s}{S_w} k_n \frac{\sin k_n \ell \cos k_c L_j + \alpha \cos k_n \ell \sin k_c L_j}{\cos k_n \ell \cos k_c L_j - \alpha \sin k_n \ell \sin k_c L_j}, \quad (2)$$

with $\alpha = S k_c / (s k_n)$, where S_w, S and s are the areas of the main waveguide of the cavity and the neck, respectively. ℓ and L_j denote the lengths of the neck and of the cavity of the j th resonator, respectively (see Fig. 1(b)). The wavenumbers are $k_m = k[1 + \beta \delta / R_m]$, with $m = w, c, n$ (waveguide, cavity, and neck respectively) and R_m the corresponding radius, with $\beta = [1 + (\gamma - 1) \text{Pr}^{-1/2}](1 + i) / \sqrt{2}$, where Pr is the Prandtl number at atmospheric pressure and $\gamma = 1.4$ is the heat capacity ratio of air. $\delta = \sqrt{\nu / \omega}$ is the viscous boundary layer depth (ν the kinematic viscosity of air). The term proportional to β in the wavenumber k is a good model for the viscous and thermal attenuation of sound in the duct. We notice that with $s \ll S_w$, the strength of the Helmholtz scatterer is small except at resonances.

Setting L as the cavity length of the ordered case, approximating k_n and k_c by k , and thus omitting the attenuation, these cavity resonances correspond to a vanishing term

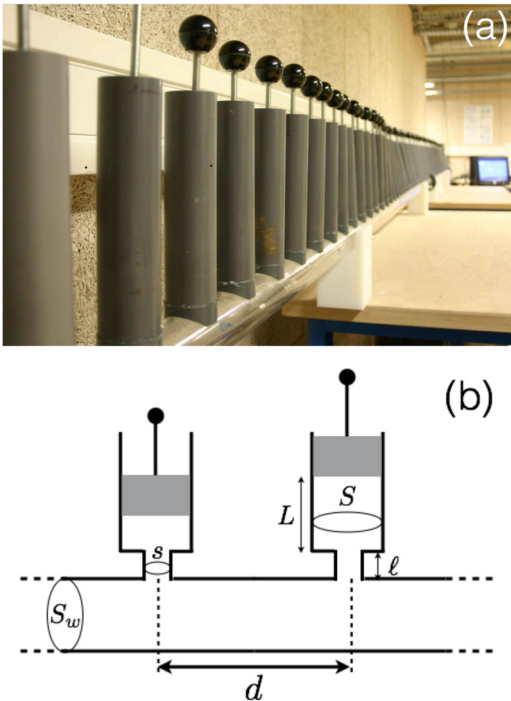


FIG. 1. (a) Picture of the experimental set up. (b) Schematic of the experimental setup.

$D(k) \equiv \cos k \ell \cos k L - \alpha \sin k \ell \sin k L$, and they are of two types: (i) the typical Helmholtz resonance occurring at low frequency, say for $k \ell \rightarrow 0$ close to $k_H = 1 / \sqrt{\alpha \ell L}$ and (ii) the resonances in the cavity (hereafter referred as volume resonances), near $k L = q \pi$ with integer q . For instance, for $q = 1$,

$$k_V L = \pi + \frac{1}{\alpha \tan(\pi \ell / L)}. \quad (3)$$

For a single resonator, these resonances produce a vanishing transmission. When the resonators are organized in a perfectly periodic array, band gaps are created around the resonance frequencies, according to Bloch Floquet wavenumber Q becoming purely imaginary, Q being given by

$$\cos Q d = \cos k d + \frac{V}{2k} \sin k d, \quad (4)$$

where $V \equiv V_j(L_j = L)$. When disorder is introduced in the volume cavity by changing the length L_j of the j th cavity, $L_j = L(1 + \epsilon_j)$ with L the mean value of the cavity length and $\epsilon_j \in [-\epsilon/2; \epsilon/2]$, it is possible to predict the new Bloch Floquet wavenumber K using the CPA approach¹² (see Appendix B for details)

$$\cos K d = \cos k d + \frac{\langle V \rangle}{2k} \sin k d, \quad (5)$$

where $\langle \cdot \rangle$ denotes the ensemble average for all realizations of the $\{\epsilon_j\}_j$ -values. For a lattice of N cells, the resulting transmission coefficient is

$$T_N = e^{-ikNd} \frac{e^{ikd} - B^2 e^{-ikd}}{e^{ikd-iKNd} - B^2 e^{-ikd+iKNd}}, \quad (6)$$

where we have written $p(x \geq Nd) = T_N e^{ik(x-Nd)}$ (the incident wave is e^{ikx}) and with

$$B \equiv \frac{e^{i(k-K)d} - 1}{1 - e^{-i(k+K)d}}. \quad (7)$$

Obviously, the above results obtained from CPA recover the perfectly periodic case when $\epsilon = 0$.

In the following, we present the experimental set-up to realize the lattice of Helmholtz resonators. Comparisons between the measured transmission and the above CPA result, Eq. (6), are presented.

III. EXPERIMENTAL RESULTS

A. Experimental set-up

The experimental set-up (Fig. 1) consists of a 8 m long cylindrical waveguide with an inner area $S_w = 2 \times 10^{-3} \text{ m}^2$ and a 0.5 cm thick wall. This waveguide is connected to an array of $N = 60$ Helmholtz resonators periodically distributed, with inter resonator distance $d = 0.1 \text{ m}$. Each resonator is composed of a neck (cylindrical tube with an inner area $s = 7.85 \times 10^{-5} \text{ m}^2$ and a length $\ell = 2 \text{ cm}$) and by a cavity with variable length. The cavity is a cylindrical tube with an

inner area $S = 1.4 \times 10^{-3} \text{ m}^2$ and a maximum length $L_{max} = 16.5 \text{ cm}$, see Fig. 1(b).

The sound source is connected to the input of the main tube. The source is embedded in an impedance sensor,²⁴ allowing the measurement of the input impedance of the lattice Z , defined as the ratio of the acoustic pressure p and the acoustic flow u (the product of the velocity by the area cross section) at the entrance of the lattice, as described in Refs. 20 and 25.

This permits determination of the reflection coefficient R defined as $p = (1 + R)p^+$ owing to $u = u^+ + u^-$ with $u^+ = p^+/Z_w$, $u^- = -p^-/Z_w$, where the index $+$ and $-$ denote the parts of the quantity associated with right- and left-going waves

$$R = \frac{Z - Z_w}{Z + Z_w}. \quad (8)$$

At the output, an anechoic termination made of a 10 m long waveguide partially filled with porous plastic foam suppresses the back-propagating waves. This ensures the output impedance to be close to the characteristic impedance $Z_w = \rho c/S_w$. Finally, a microphone is used to measure the pressure p_e at the end of the lattice.

Using line matrix theory, (p, u) and (p_e, u_e) are linked by the transfer matrix through

$$\begin{pmatrix} p \\ u \end{pmatrix} = \begin{pmatrix} A & B \\ C & D \end{pmatrix} \begin{pmatrix} p_e \\ u_e \end{pmatrix}, \quad (9)$$

with $p = Zu$ (Z being measured) and $u_e = p_e/Z_w$ (the acoustic flow is deduced from p_e because of the anechoic termination). Then, the transmission coefficient T defined as $p_e = Tp^+$ is calculated using that $u = (1 + R)p^+/Z$ by definition of R and from above, $u = [C + D/Z_w]p_e = [C + D/Z_w]Tp^+$, from which

$$T = \frac{2Z_t}{Z + Z_w}, \quad (10)$$

where $Z_t \equiv [C + D/Z_w]^{-1}$ is deduced from the measured (p_e, u) -values.

When considered, the disorder in the lattice is introduced through the variable lengths $L_j, j = 0, \dots, N$ of the cavities, and $L_j = L(1 + \epsilon_j)$ is used with a normal distribution of

ϵ_j being chosen for each realization and for each resonator cavity, with $\epsilon_j \in [-\epsilon/2; \epsilon/2]$, resulting in a variable scattering strength, V_j in Eq. (2). The transmission coefficients are measured for 10 different distributions with same standard deviation, and the mean value $\langle T \rangle$ is taken.

B. Experimental observations

The transmission coefficient T in the perfect periodic case is presented in Fig. 2 for a cavity length $L = 0.165 \text{ m}$. Four band gaps are visible: The first (labeled a) at low frequency is associated with the Helmholtz resonance (k_H) for $kd/\pi \in [0.15; 0.25]$, corresponding to frequency in [300; 450] Hz. Two other band gaps (labeled b and d) are associated with the two first volume resonances (kL close to π and 2π); these are for kd/π in [0.64; 0.68], [1.22; 1.24] (corresponding frequency ranges [1110; 1170] Hz, and [2100; 2150] Hz). These three band gaps associated with resonances of the scatterers are often referred as hybridization band gaps.¹⁵ Finally, the band gap labeled c is associated with the Bragg resonance, for $kd/\pi \in [1; 1.03]$, (frequency range [1700; 1800] Hz). This band structure has been described in detail, including non linear aspects, in Refs. 21–23. The comparison between the experimental result (blue line) and the analytical expression (red line), Eq. (6), shows a good agreement. The discrepancy in the low frequency regime may be attributable to the bad quality of the source in this frequency range.

Finally, the strong peaks appearing in the experimental measurements are due to the imperfection in the anechoic termination, resulting in interferences between forward and backward waves in the main tube.

Fig. 3(a) shows the transmission in the perfectly periodic case for $L = 0.1 \text{ m}$. With $L = d$, the volume resonance k_V , with $k_V \sim \pi/L$, and the Bragg frequency $k_B = \pi/d$ are very close, resulting in an almost perfect overlap (the perfect overlap is defined by $k_V = k_B$) of the two corresponding band gaps, previously labeled b and c, visible here in the range $kd/\pi \in [0.98; 1.12]$ (frequency range [1600; 1800] Hz). The first band gap, associated with the Helmholtz resonance k_H is almost unaffected by the change in L while the volume resonance with $k_V L \simeq 2\pi$ (previously labeled d) is sent to higher frequency (not visible in our plot). A noticeable feature is the existence of a small transparency band inside the large

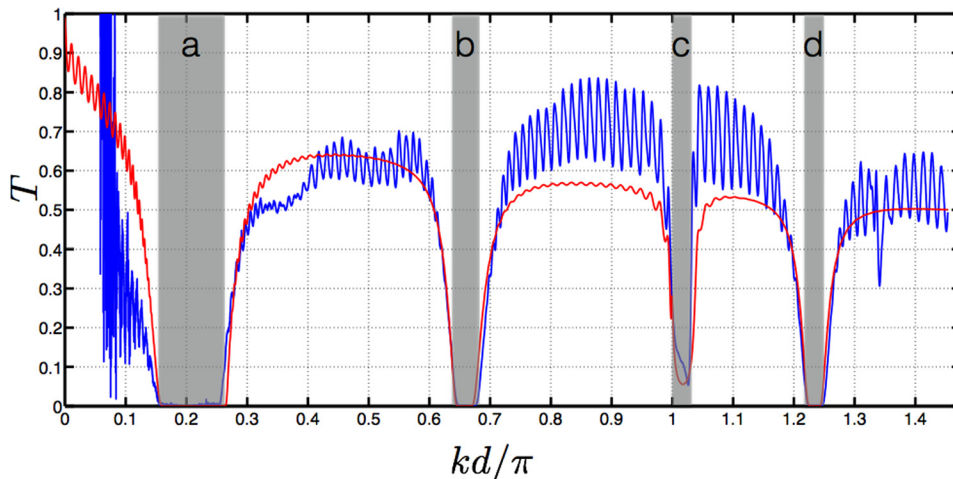


FIG. 2. Transmission coefficient for an ordered lattice with a cavity length $L = 0.165 \text{ m}$ and lattice spacing $d = 0.1 \text{ m}$. Blue line corresponds to the experimental measurement and red line corresponds to the analytical prediction, Eq. (6).

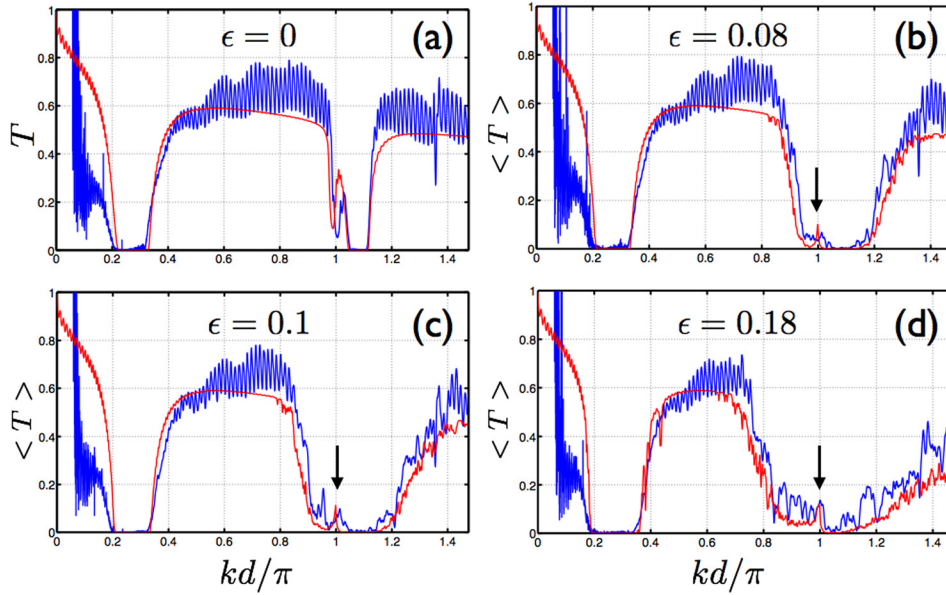


FIG. 3. (a) Transmission coefficient of an ordered lattice for a cavity length $L=0.1$ m and lattice spacing $d=0.1$ m. (b) Mean value of the transmission coefficient for a disordered lattice with $\epsilon=0.08$. (c) Mean value of the transmission coefficient for a disordered lattice with $\epsilon=0.1$. (d) Mean value of the transmission coefficient for a disordered lattice with $\epsilon=0.18$. The blue line corresponds to the experimental case obtained with 10 averages and the red line corresponds to our analytical prediction with 100 averages (except for (a) without disorder).

stop band near $kd=\pi$, a feature already observed in other systems where such overlapping is realized.^{16,17,20} This feature, in addition to the main behavior of T , is accurately captured by our analytical expression, Eq. (6), in the perfectly periodic case, thus with constant unperturbed potential V (and $K=Q$).

We now consider several amplitudes ϵ of disorder in the scattering strength of the resonators with a mean value of the cavity length $L=0.1$ m, as previously described. The measured transmission coefficients $|\langle T \rangle|$ are reported in Figs. 3(b)–3(d) for, respectively, $\epsilon=0.08$, $\epsilon=0.1$, and $\epsilon=0.18$.

As expected, the more visible effects of the disorder are (i) to strengthen the opacity in the pass band and (ii) to enlarge the band gap width. This is associated with the fact that the wavenumber K of the effective Bloch mode acquires an imaginary part due to the disorder (in addition to the attenuation) in the pass bands of the perfectly ordered case. In counterpart, in the stop bands of the perfectly ordered case, the imaginary part of the wavenumber decreases, resulting in an increase in the transmission.⁶

In the second stop band, an interesting behavior can be noticed, although very qualitative at this stage: inside the second band gap, around $kd/\pi=1$, the small transparency band remains visible (marked by arrow in Figs. 3(b)–3(d)), since we observe a peak of transmission robust to disorder. This trend is confirmed by the analytical model (red curves on Fig. 3).

In Sec. IV, we use numerical calculations to get further insights on this induced transparency near $kd/\pi=1$.

IV. NUMERICAL INTERPRETATION OF THE INDUCED TRANSPARENCY

We now present results from numerical experiments of the propagation in the array of Helmholtz resonators. This is done by solving Eq. (1), with various V_j values. The disorder is introduced by using $L_j=L(1+\epsilon_j)$ in Eq. (2). To calculate $p(x)$, we implement a method based on the impedance, as described in Ref. 9. For each frequency, $N_r=10^4$ realizations of the disorder with same amplitude ϵ are performed. The effective transmission $\langle T \rangle$ is calculated by averaging the

transmission coefficients $\langle T \rangle = 1/N_r \sum T_r$, where the T_r is the transmission coefficient for each realization.

The main result is presented in Fig. 4. In Fig. 4(a), $|\langle T \rangle|$ is shown in a 2D plot as a function of $kd/\pi \in [0.7; 1.3]$ (around the Bragg frequency) and $\epsilon \in [0; 0.3]$. Fig. 4(b) shows several transmission curves for given ϵ -values ($\epsilon =$

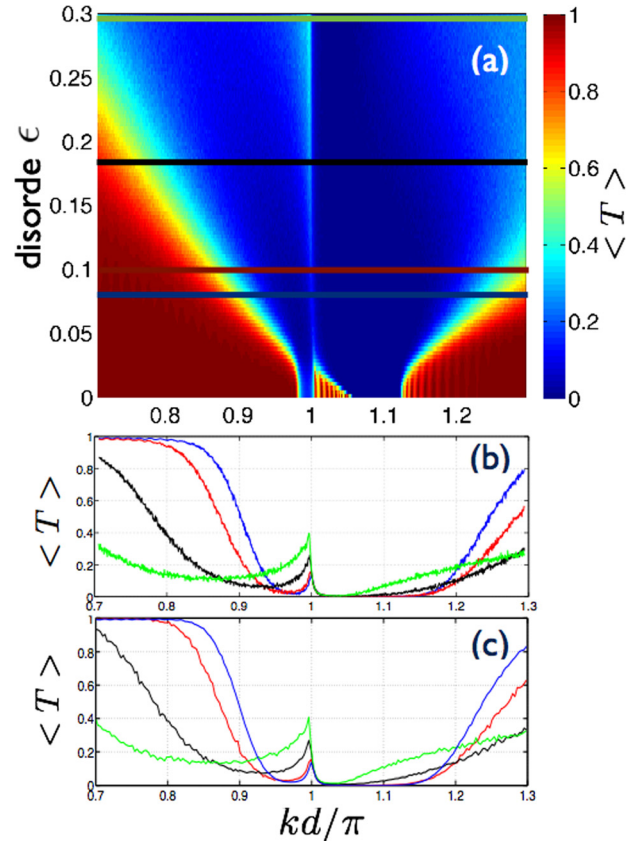


FIG. 4. (a) Full numerical simulation of the mean value of the transmission coefficient as a function of the disorder. (b) Full numerical simulation of the mean value of the transmission coefficient for $\epsilon=0.08$ (blue), $\epsilon=0.1$ (red), $\epsilon=0.18$ (black), and $\epsilon=0.3$ (green). (c) Analytical prediction of the mean value of the transmission coefficient for $\epsilon=0.08$ (blue), $\epsilon=0.1$ (red), $\epsilon=0.18$ (black), and $\epsilon=0.3$ (green).

0.08, 0.1, 0.18, 0.3) computed numerically. We have verified that the number of realizations is sufficient to get a converged average value of transmission. Fig. 4(c) presents averaged transmission data for the same ϵ -values obtained by analytical CPA method (in this case, the average of V (Eq. (2)) obtained with a number of realizations $N_r = 10^7$). The transparency robust to disorder is quantitatively confirmed: For the largest values of disorder, results from the full numerical simulation and analytical CPA method show clearly that the transmission near $kd/\pi = 1$ increases with the disorder.

V. DISCUSSION

The robustness of transparency to disorder could appear counterintuitive with regards to the usual influence of disorder in wave propagation. Indeed, on average, the presence of disorder is known to be unfavorable for the wave propagation and to decrease the transmission. In this study, the robustness of transparency is the result of the mixing of two different physical phenomena: (1) the non-exact overlap of the Bragg and hybridization band gaps which generates, in the periodic case, a narrow passband located inside a band gap and (2) the presence of disorder on potential which prevents the wave propagation inside the media.

In the periodic case, one of the edges of the narrow transparency band due to overlap is located at $kd/\pi = 1$ which corresponds to the Bragg frequency.^{16,20} With disorder, the physical understanding of the band gap modification in case of overlap remains currently an open question. It appears that the lower edge of the transparency band is the least affected by the disorder. Indeed, in Fig. 4, we observe that the transparency band disappears except in the vicinity of its lower edge near $kd/\pi = 1^-$. Moreover, the transmission in this region increases with the disorder strength.

VI. CONCLUSION

In this paper, we report an experimental and numerical characterizations of a periodic-on-average disordered system. The usual widening of the band gaps of disordered arrays is observed. On the other hand, when nearly perfect overlap between the Bragg and the scatterer resonance frequencies is realized, evidence of robust transparency has been shown.

ACKNOWLEDGMENTS

This study has been supported by the Agence Nationale de la Recherche through the grant ANR ProCoMedia, Project No. ANR-10-INTB-0914. V.P. thanks the support of Agence Nationale de la Recherche through the grant ANR Platon, Project No. ANR-12-BS09-0003-03.

APPENDIX A: DERIVATION OF THE POTENTIAL V

We consider a small control volume in the tube (grey part in Fig. 5). Since the wavelength is much larger than the control volume, we have continuity of the pressure $p^+ = p^- = p$ (Ref. 26) (and also $p_C = p$). To obtain the value of $[p']$ (and $p' = \partial_x p$), we get, by continuity of the flux

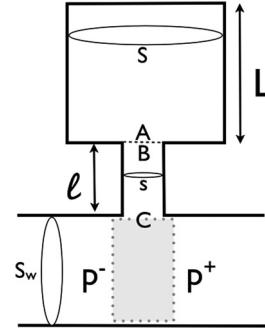


FIG. 5. Geometry of the Helmholtz resonator connected to the central waveguide at C. The control volume is in grey.

$$\partial_x p^+ - \partial_x p^- = -s/S_w \partial_y p_C, \quad (\text{A1})$$

and we have to find $\partial_y p_C$ as a function of p , at the point C. The wave equation inside the cavity with hard walls implies that

$$\partial_y p_A/p_A = k_c \tan(k_c L), \quad (\text{A2})$$

where L is the length of the cavity (Fig. 5). Then, conservation of the pressure and flow rate between points A and B give

$$s \partial_y p_B/p_B = S \partial_y p_A/p_A. \quad (\text{A3})$$

The wave propagation inside the neck gives (by transfer matrix for instance)

$$\partial_y p_C/p_C = \frac{k_n \sin(k_n \ell) + \cos(k_n \ell) \partial_y p_B/p_B}{\cos(k_n \ell) - \sin(k_n \ell)/k_n \partial_y p_B/p_B}, \quad (\text{A4})$$

so that $\partial_y p_C/p = Y$ with

$$Y = k_n \frac{sk_n \sin(k_n \ell) \cos(k_c L) + \cos(k_n \ell) S k_c \sin(k_c L)}{sk_n \cos(k_n \ell) \cos(k_c L) - \sin(k_n \ell) S k_c \sin(k_c L)}. \quad (\text{A5})$$

Eventually, Eq. (A1) becomes

$$\partial_x p^+ - \partial_x p^- = -s/S_w Y p, \quad (\text{A6})$$

and the wave equation in the waveguide can be written as

$$p'' + k^2 p = V \delta(x) p(x), \quad (\text{A7})$$

with

$$V = -\frac{s}{S_w} Y = -\frac{sk_n \sin(k_n \ell) \cos(k_c L) + \cos(k_n \ell) S k_c \sin(k_c L)}{S_w sk_n \cos(k_n \ell) \cos(k_c L) - \sin(k_n \ell) S k_c \sin(k_c L)}. \quad (\text{A8})$$

APPENDIX B: CPA CALCULATION

In this Appendix, we adapt the results of Ref. 12 to the present situation to obtain Eqs. (5)–(7). The main differences concern a different definition of the potential (by a factor $2k$) and the fact that the potential without disorder in Ref. 12 corresponds to the averaged potential, which is not the case in the present study.

First, we report the equations in Ref. 12 that are needed (all the terms coming from Ref. 12 are written with the symbol tilde). The dispersion relation is derived

$$\text{from [12]} \begin{cases} \text{After Eq. [12](1),} & \tilde{V}_j = \tilde{V}(1 + \xi_j), \text{ with } \langle \xi_j \rangle = 0, \\ \text{Eqs. [12](14),} & \cos \tilde{Q}d = \cos kd + \tilde{V} \sin kd, \text{ for all } V_j = \langle \tilde{V}_j \rangle, \\ \text{Eq. [12](20),} & \cos Kd = \cos \tilde{Q}d + O(\xi^2). \end{cases} \quad (\text{B1})$$

In the third equation of (B1), $\xi^2 \equiv \langle \xi_n^2 \rangle / 12$, and we have used in Eq. (20) in Ref. 12 that $t_\xi = O(\xi^2)$; see the expression of t_ξ after Eq. (25) in Ref. 12. Then, the transmission coefficient is derived; we report below the result in the case of disorder in the strength of the scattering ξ without disorder in the potential ($\epsilon = 0$),

Transmission coefficient, from [12]

$$\begin{cases} \text{Eq. [12](37),} & T_N = e^{iknd} \frac{e^{ikd} - \mathcal{B}^2 e^{-ikd}}{e^{ikd-iKNd} - \mathcal{B}^2 e^{-ikd+iKNd}}, \\ \text{with Eq. [12](28), } \epsilon = 0, & \mathcal{B} = \frac{e^{i(k-K)d} - 1}{1 - e^{-i(k+K)d}}. \end{cases} \quad (\text{B2})$$

Next, we show the correspondences between the potentials V in Eq. (1) and \tilde{V} in Eq. [12](1) and the average values of the potential: $2k\tilde{V}_j = V_j$, from which $2k\tilde{V} = \langle V \rangle$ and $2kV\xi_n = \delta V_n$. The above equations (B1) and (B2) become

Dispersion relation

$$\begin{cases} V_j = \langle V \rangle + \delta V_j, \text{ with } \langle \delta V_j \rangle = 0, \\ \cos \tilde{Q}d = \cos kd + \frac{\langle V \rangle}{2k} \sin kd, \text{ for all } \delta V_j = 0, \\ \cos Kd = \cos kd + \frac{\langle V \rangle}{2k} \sin kd + O(\delta V^2), \end{cases} \quad (\text{B3})$$

and Eq. (B2) remains unchanged.

The third equation of (B3) and Eq. (B2) correspond to Eqs. (5)–(7) in the text of the paper.

As a final remark, note that \tilde{Q} in the second equation of Eq. (B3) differs from Q defined in Eq. (4). Indeed, \tilde{Q} is the Floquet wavenumber of a periodic array with all the scatterers having the average scattering strength $\langle V \rangle$, while Q is the

Floquet wavenumber of the periodic array with all the scatterers having the scattering strength with $L_j = L$ (and $V(L_j = L) \neq \langle V \rangle$).

¹V. Romero-Garcia, C. Lagarrigue, J.-P. Groby, O. Richoux, and V. Tournat, *J. Phys. D* **46**, 305108 (2013).

²M. I. Hussein, K. Hamza, G. M. Hulbert, and K. Saitou, *Waves Random Complex Media* **17**, 491 (2007).

³T. Z. Wu and S. T. Chen, *IEEE Trans. Microwave Theory Tech.* **54**, 3398 (2006).

⁴J. H. Page, A. Sukhovich, S. Yang, M. L. Cowan, F. Van Der Biest, A. Tourin, M. Fink, Z. Liu, C. T. Chan, and P. Sheng, *Phys. Status Solidi B* **241**, 3454 (2004).

⁵C. M. Linton and P. A. Martin, *J. Acoust. Soc. Am.* **117**(6), 3413–3423 (2005).

⁶V. D. Freilikher, B. A. Liansky, I. V. Yurkevich, A. A. Maradudin, and A. R. McGurn, *Phys. Rev. E* **51**(6), 6301 (1995).

⁷L. I. Deych, D. Zaslavsky, and A. A. Lisyansky, *Phys. Rev. Lett.* **81**(24), 5390 (1998).

⁸P. Han and C. Zheng, *Phys. Rev. E* **77**(4), 041111 (2008).

⁹A. Maurel and V. Pagneux, *Phys. Rev. B* **78**(5), 052301 (2008).

¹⁰A. Maurel, P. A. Martin, and V. Pagneux, *Waves Random Complex Media* **20**(4), 634–655 (2010).

¹¹F. M. Izrailev, A. A. Krokhin, and N. M. Makarov, *Phys. Rep.* **512**(3), 125–254 (2012).

¹²A. Maurel and P. A. Martin, *Eur. Phys. J. B* **86**(11), 1–10 (2013).

¹³S. H. Chang, H. Cao, and S. T. Ho, *IEEE J. Quantum Electron.* **39**(2), 364–374 (2003).

¹⁴Y. Xu, Y. Li, R. K. Lee, and A. Yariv, *Phys. Rev. E* **62**, 7389 (2000).

¹⁵C. Croenne, E. J. S. Lee, H. Hu, and J. H. Page, *AIP Adv.* **1**, 041401 (2011).

¹⁶N. Sugimoto and T. Horioka, *J. Acoust. Soc. Am.* **97**(3), 1446 (1995).

¹⁷C. E. Bradley, *J. Acoust. Soc. Am.* **96**(3), 1844 (1994).

¹⁸Y. Xiao, B. R. Mace, J. Wen, and X. Wen, *Phys. Lett. A* **375**, 1485 (2011).

¹⁹N. Kaina, M. Fink, and G. Lerosey, *Sci. Rep.* **3**, 3240 (2013).

²⁰G. Theocharis, O. Richoux, V. Romero-Garcia, A. Merkel, and V. Tournat, *New J. Phys.* **16**, 93017 (2014).

²¹O. Richoux and V. Pagneux, *Europhys. Lett.* **59**(1), 34 (2002).

²²O. Richoux, E. Morand, and L. Simon, *Ann. Phys.* **324**(9), 1983–1995 (2009).

²³O. Richoux, V. Tournat, and T. LeVanSuu, *Phys. Rev. E* **75**(2), 026615 (2007).

²⁴The sensor is developed jointly by CTTM (Centre de Transfert de Technologie du Mans, Le Mans, France) and LAUM (Laboratoire d'Acoustique de l'Université du Maine, Le Mans Cedex, France).

²⁵C. A. Macaluso and J. P. Dalmont, *J. Acoust. Soc. Am.* **129**(1), 404–414 (2011).

²⁶A. D. Pierce, *Acoustics: An Introduction to Its Physical Principles and Applications* (Acoustical Society of America, 1989).